

## **Development and Validation of an Unsaturated Soil Water Flow Model for Oil Palm**

**Teh, C. B. S.**

*Department of Land Management, Faculty of Agriculture, Universiti Putra Malaysia, 43400 UPM, Serdang, Selangor, Malaysia*

### **ABSTRACT**

The development and use of a soil water model to predict the soil water flow and content under oil palm would be useful as a tool for more effective oil palm water management. Although many soil water models exist, none of them has been specifically developed, applied, and validated for oil palm. Consequently, the purpose of this study is to develop and validate such a model. Water flow was modelled following a one-dimensional “tipping bucket” system, and the soil profile was divided into several soil layers where the soil water and hydraulic characteristics for each layer were estimated based on the soil carbon content and soil texture. Darcy’s law was applied to estimate the various soil water fluxes. The soil water model included algorithms to estimate the root water uptake and water stress response by oil palm. Raw data of measured soil water content for several soil depths (up to 90 cm) from two studies (Moraidi et al., 2015; Nur Farahin, 2013) were obtained, so that the accuracy of the soil water model could be validated by comparing simulations of soil water content with measured values. The model was satisfactorily accurate, showing similar daily trend as that observed for the measured soil water content. Goodness-of-fit indexes further indicated that the model simulations showed little to no overall model bias and with an average absolute prediction error of only 10%. Future work is to increase model accuracy by estimating the daily actual evapotranspiration instead as assumed constant in this study.

*Keywords:* Darcy’s law, model, oil palm, soil moisture, water flow

### **ARTICLE INFO**

*Article history:*

Received: 4 October 2017

Accepted: 8 December 2017

*E-mail address:*

cbsteh@yahoo.com (Teh, C. B. S.)

### **INTRODUCTION**

Oil palm irrigation studies as reviewed by Corley and Tinker (2016), have shown that despite the large annual rainfall amount in Malaysia, oil palm yields in the country

could further increase by an average of between 2 to 30% with additional supply of water through irrigation. At times, oil palm annual yields can increase by 100%, as reported by Lee and Izwanizam (2013). Oil palm yields respond to irrigation because Malaysia’s annual distribution of rainfall is not constant, with notable dry periods in particular during the middle of the year. It is during such dry periods that oil palm risks suffering from water stress. Oil palm water stress is a function of several factors, one of which is the amount of water available in the soil for the crop, where Carr (2011) reported that for every 100 mm of potential soil water deficit, oil palm yields would decrease by approximately 10%.

Consequently, the development and use of a mathematical model for simulating and predicting water movement and content in soils under oil palm would be useful for oil palm studies and as a tool for more effective oil palm water management. Despite the development of many soil water models (e.g., Clemente et al., 1994), none of them

has been specifically applied nor their simulation accuracy validated for oil palm. Therefore, the main purpose of this paper is to present the development and validation of a soil water model specifically for oil palm, for simulating the soil water movement and soil water content in the vadose (unsaturated) zone of the soil, which is part of a larger ongoing study. The future goal of the ongoing study is to produce a more comprehensive oil palm growth and yield model by incorporating the soil water model with other model components involving energy balance, meteorology, and oil palm growth and yield.

**MATERIALS AND METHODS**

**Soil Water Model Development**

Water flow was modeled following the ‘tipping bucket’ system, where water flow is treated in a sequential manner, beginning from the first soil layer, then moving successively down to the last soil layer (Hillel, 1977), as shown in Figure 1.

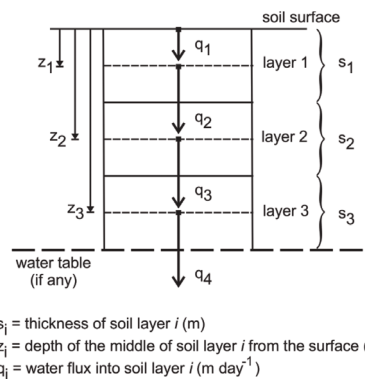


Figure 1. Water flow in a soil profile

In this case, this soil profile is divided into three successive layers. The presence of a water table, if any, is always just beneath the last (in this case, third) soil layer

The whole soil profile was divided into two or more consecutive layers, with first soil layer as a relatively thin layer, and the second layer covering up to at least the entire rooting depth. Soil layer  $i$  ( $i = 1$  to  $N$ , where  $N$  is the total number of soil layers) has a thickness of  $s_i$  (m), and the depth from the soil surface to the middle of layer  $i$  is  $z_i$ . Water flux into soil layer  $i$  is denoted as  $q_i$  (m day<sup>-1</sup>).

Water flow follows the downward positive coordinate system, where the downward and upward direction of water flow is taken as a positive and negative value respectively, and the reference level is taken as the soil surface level. Darcy's law is used to describe the water flow in the soil. Water flow is taken to occur from the middle of layer  $i - 1$  to the middle of layer  $i$ . Water flux into soil layer  $i$  is:

$$q_i = \begin{cases} P_{net} - ET_s - ET_{c,i} & i = 1 \\ \frac{K_{\theta,i}}{z_i - z_{i-1}} (H_i - H_{i-1}) - ET_{c,i} & 1 < i \leq N \\ K_{\theta,N} & i = N + 1 \end{cases} \quad [1a]$$

$$\overline{K_{\theta,i}} = \frac{K_{\theta,i-1} - K_{\theta,i}}{\ln K_{\theta,i-1} - \ln K_{\theta,i}} \quad [1b]$$

where  $q$  is the water flux (m day<sup>-1</sup>);  $P_{net}$  is the net daily rainfall (m day<sup>-1</sup>);  $ET_s$  is the actual daily soil evaporation (which occurs only from the first soil layer) (m day<sup>-1</sup>);  $ET_c$  is the daily extraction of water by roots (actual plant transpiration) (m day<sup>-1</sup>);  $\overline{K_{\theta,i}}$  is the logarithmic mean of the hydraulic conductivities of layer  $i$  and  $i - 1$  (m day<sup>-1</sup>);  $z$  is the soil layer's depth (m); and  $H$  is the total head (matric suction and

gravity heads) (m). Note that water table, if present, is treated as an additional but saturated soil layer  $N+1$ , and Eq. 1 used to describe the capillary rise of water.

Water flux out of the last soil layer ( $i = N$ ) is denoted by  $q_{N+1}$ , and without the presence of a water table, it is merely equal to  $K_{q,N}$  because it is assumed that the soil below the last layer is uniformly wet and has the same water content as the last soil layer. Consequently, water flux is only due to gravity gradient (no matric suction gradient). In this case,  $q_{N+1} = K_{q,N}$ .

The net flux  $\hat{q}_i$  (m day<sup>-1</sup>) in soil layer  $i$  is the difference between incoming  $q_i$  and outgoing water  $q_{i+1}$  fluxes:

$$\hat{q}_i = q_{i-1} - q_{i+1} \quad [2]$$

where a positive net flux means soil water content has increased, and in contrast, a negative net flux denotes the soil is drying. This means that the change in the soil water content is determined by:

$$Q_{i,t+1} = Q_{i,t} + \hat{q}_i \quad [3]$$

where  $Q_{i,t}$  and  $Q_{i,t+1}$  are the water content in soil layer  $i$  (m) between two successive time steps  $t$  and  $t+1$ , respectively.

For each soil layer  $i$ , the volumetric soil water content (m<sup>3</sup> m<sup>-3</sup>) at permanent wilting point  $\theta_{1500}$ , field capacity  $\theta_{33}$ , and saturation  $\theta_0$  were estimated from the soil's texture and organic matter content based on empirical equations by Saxton and Rawls (2006):

$$\theta_{1500} = \theta_{1500t} + (0.14\theta_{1500t} - 0.02)$$

$$\theta_{1500t} = -0.024S + 0.487C + 0.006OM + 0.005(S \times OM) - 0.013(C \times OM) + 0.068(S \times C) + 0.031 \quad [4b]$$

$$\theta_{33} = \theta_{33t} + (1.283\theta_{33t}^2 - 0.374\theta_{33t} - 0.015) \quad [5a]$$

$$\theta_{33t} = -0.251S + 0.195C + 0.011OM + 0.006(S \times OM) - 0.027(C \times OM) + 0.452(S \times C) + 0.299 \quad [5b]$$

$$\theta_0 = \theta_{33} + \theta_{(0-33)} - 0.097S + 0.043 \quad [6a]$$

$$\theta_{(0-33)} = \theta_{(0-33)t} + 0.636\theta_{(0-33)t} - 0.107 \quad [6b]$$

$$\theta_{(0-33)t} = 0.278S + 0.034C + 0.022OM - 0.018(S \times OM) - 0.027(C \times OM) - 0.584(S \times C) + 0.078 \quad [6c]$$

where *S* and *C* are the sand and clay contents, respectively (fraction); and *OM* is the organic matter content (%).

The method by Bittelli et al. (2015) was followed to estimate the hydraulic conductivity for unsaturated ( $K_{q,i}$ ; m day<sup>-1</sup>) and saturated flow ( $K_{s,i}$ ; m day<sup>-1</sup>) in soil layer *i* as:

$$K_{\theta,i} = K_{s,i} (\theta_i / \theta_{0,i})^{3+2/\lambda} \quad [7]$$

$$K_{s,i} = 864 \times 0.07 \times \{\theta_{0,i} - [1 - (\psi_e/33)^\lambda]\}^4 \quad [8]$$

where  $q_i$  and  $\theta_{0,i}$  are the current soil water content and saturation soil water content (m<sup>3</sup> m<sup>-3</sup>) in soil layer *i*, respectively; *l* is the slope of the logarithmic suction-soil moisture curve; and  $\psi_e$  is the air-entry suction (kPa), and they are determined by

$$\lambda = [8.25 - 1.26 \ln(d_g)]^{-1} \quad [9]$$

$$\psi_e = 3.9 - 0.61 \ln(d_g) \quad [10]$$

$$d_g = \exp[-1.96C + 2.3(1 - S - C) + 5.76S] \quad [11]$$

where  $d_g$  is the geometric mean distribution ( $\mu\text{m}$ ) of the soil's particles sizes; and *C* and *S* are the clay and sand fractions, respectively.

The soil matric suction head ( $H_{m,i}$ ; m) and gravity head ( $H_{g,i}$ ; m) in soil layer *i* are determined by

$$H_{m,i} = \begin{cases} 3.3 - \left[ \frac{(33 - \psi_e)(\theta_i - \theta_{33,i})}{10(\theta_{0,i} - \theta_{33,i})} \right] & \theta_i \geq \theta_{33,i} \\ \frac{\exp(\ln 33 + \frac{1}{\lambda} \ln \theta_{33,i})}{10\theta_i^{1/\lambda}} & \theta_i < \theta_{33,i} \end{cases} \quad [12]$$

$$H_{g,i} = z_i \quad [13]$$

where  $z_i$  is the depth of the middle of soil layer *i* from the soil surface (m).

Actual soil evaporation  $ET_s$  (taken as m day<sup>-1</sup>) was calculated from Teh (2006), and van Keulen and Seligman (1987) as

$$ET_s = PET_s \times R_{Ds} \quad [14a]$$

$$R_{Ds} = \frac{1}{1 + (3.607\theta_1/\theta_{s,1})^{-9.3172}} \quad [14b]$$

where  $PET_s$  is the potential evaporation ( $m\ day^{-1}$ );  $R_{Ds}$  is the reduction factor for evaporation (ranging from 0 to 1); and  $q_i$  and  $q_{s,i}$  are the current and saturated soil water content, respectively, for the first soil layer ( $i = 1$ ) (both in  $m^3\ m^{-3}$ ).

Actual transpiration ( $ET_c$ ,  $m\ day^{-1}$ ) was calculated from Kropff (1993) as

$$ET_c = PET_c \times R_{Dc} \quad [15a]$$

$$R_{Dc} = \begin{cases} 1 & \theta_{root} \geq \theta_{cr,root} \\ \frac{\theta_{root} - \theta_{1500,root}}{\theta_{cr,root} - \theta_{1500,root}} & \theta_{1500,root} < \theta_{root} < \theta_{cr,root} \\ 0 & \theta_{root} \leq \theta_{1500,root} \end{cases} \quad [15b]$$

$$\theta_{cr,root} = \theta_{1500,root} + p(\theta_{0,root} - \theta_{1500,root}) \quad [15c]$$

where  $PET_c$  is the potential transpiration;  $R_{Dc}$  is the reduction factor for transpiration (0 to 1);  $q_{root}$  is the soil water content currently in the root zone;  $\theta_{1500,root}$  and  $\theta_{0,root}$  are the soil root zone's permanent wilting point and saturation, respectively; and  $q_{cr,root}$  is the volumetric water content in the root zone below where water stress occurs. All soil water content is in  $m^3\ m^{-3}$ .

For C3 plants in general,  $p$  in Eq. 15c is often taken as 0.5. However, comparisons of the soil water content between irrigated and non-irrigated oil palm trials from 1983 to 1990 by Foong (1999) suggested that oil palm is more sensitive to water stress because  $p$  is more likely 0.6 than 0.5 of  $(\theta_{0,root} - \theta_{1500,root})$  ( $\theta_{0,root} - \theta_{1500,root}$ ). This 0.6 critical point corresponds to about half of the available soil water content (AWC) of Munchong soil series (Typic Hapludox), which was the type of soil in the oil palm

trials by Foong (1999). Similarly, fitting the best function to the data collected by Rey et al. (1998) also showed that oil palm stomatal conductance would begin to decline only when the soil water content fell below the level of about 50% of their soil's AWC (see Figure 2).

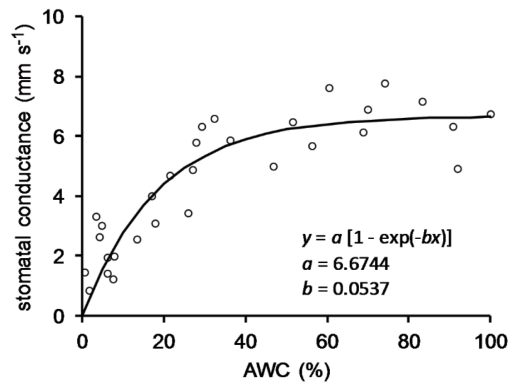


Figure 2. Fitting a Function to the Relationship between Oil Palm Leaf Stomatal Conductance and Available Soil Water Content (AWC), as measured by Rey et al. (1998). Stomatal conductance declined only when AWC was about 50% or less

The amount of water in the root zone  $q_{root}$  is the summation of water content from the first soil layer ( $i=1$ ) until the rooting depth, and the algorithm to determine  $q_{root}$  is as follows:

$$\theta_{root} = 1/d_{root} \times \sum_{i=1}^N MAX[0, \theta_i(s_i - n_i)] \quad [16a]$$

$$n_i = MAX(0, S_i - d_{root}) \quad [16b]$$

where  $d_{root}$  is the rooting depth (m);  $s_i$  is the thickness of soil layer  $i$  (m); and  $S_i$  is the cumulative thickness of soil layer  $i$  (m). Note the  $MAX$  function returns the larger of the given two values.

The amount of water extracted by roots in each soil layer is based on the measured data for oil palm by Nelson et al. (2006) and on the root water uptake algorithm by Miyazaki (2005):

$$ET_{c,i} = ET_c(\varphi_i - \varphi_{i-1}) \quad [17a]$$

$$\varphi_i = 1.8c_j - 0.8c_j^2 \quad [17b]$$

$$c_j = MIN\left[1, S_j/d_{root}\right] \quad [17c]$$

where  $S_j$  is the cumulative thickness of soil layer  $j$  (summation of thickness of the current soil layer and all its preceding soil layers). Note that  $MIN$  in Eq. 17c is the minimum function, returning the smaller of the given two values.

Lastly, net rainfall  $P_{net}$  refers to the amount of rain reaching the ground as both throughfall and stemflow. The larger the canopy cover or leaf area index, the larger the fraction of intercepted gross rainfall by the canopies and the smaller the net rainfall. Net rainfall studies on closed oil palm canopies by Lubis (2016), Chong (2012), Bentley (2007), Zulkifli et al. (2006), and Damih (1995) showed that throughfall and stemflow are on average ( $\pm$  s.e.)  $61.3 \pm 2.1$  and  $8.4 \pm 1.0\%$  of  $P_g$ , respectively ( $N = 430$  rain events).  $P_{net}$  ( $m \text{ day}^{-1}$ ) is related to oil palm leaf area index  $L$  ( $m^2 \text{ leaf } m^{-2} \text{ ground}$ ) and  $P_g$  ( $m \text{ day}^{-1}$ ) as follows:

$$P_{net} = P_g \times MAX\left[0.7295, 1 - 0.0541L\right] \quad [18]$$

where it is assumed that  $P_{net}/P_g$  decreases linearly with  $L$  until closed canopies are reached, after which  $P_{net}$  never exceeds 72.95% of  $P_g$  (Figure 3).

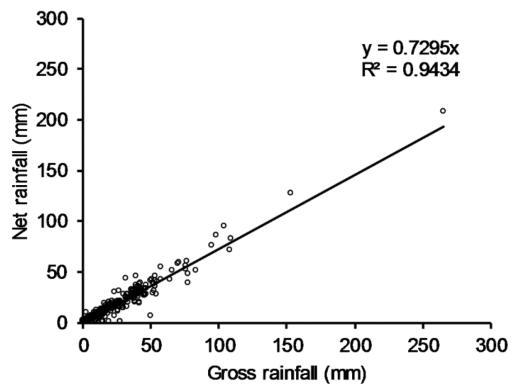


Figure 3. Strong Linear Relationship between Nett Rainfall and Gross Rainfall under Closed Oil Palm Canopies (Bentley, 2007; Chong, 2012; Damih, 1995; Lubis, 2016; Zulkifli et al., 2006) ( $N = 430$ )

### Field Data Collection

The soil water model was validated by comparing simulations with measured soil water content. Raw data of daily soil water measurements under oil palm were obtained from Nur Farahin (2013) and Moraidi et al. (2015).

The oil palm plantation in the study by Nur Farahin (2013) study was located at Universiti Putra Malaysia campus (2.9805 °N and 101.7287 °E), Serdang, and the age of the oil palms were 19 years, with a planting density of 148 palms  $ha^{-1}$ . The soil type was identified as Typic Hapludox (Munchong series). Soil water content at five random locations (over a total area of 0.1 ha) in the oil palm plantation was

measured using the AquaPro soil moisture probe (Aqua da Vinci, California). At each location, an access tube for the soil moisture probe was planted into the soil in the middle of four palms such that the soil water content for six soil depths: 0-15, 15-30, 30-45, 45-60, 60-75, and 75-90 cm could be measured. Soil water measurements were done daily at every morning. Measurements started on July 17, 2012 and ended on December 30, 2012.

Moraidi et al. (2015) collected the soil water data from the Broga oil palm estate (2.9325 °N and 101.8822 °E), located in Semenyih. The age of the oil palm was eight years, and the planting density was 156 palms ha<sup>-1</sup>. The soil type was identified as Typic Paleudult (Rengam series). Soil water content was measured in the same manner and using the same soil moisture probe as by Nur Farahin (2013) except the soil water measurements at Broga estate were done only at three random locations (over a total area of 0.22 ha) and for four soil depths: 0-15, 15-30, 30-45, and 45-60 cm. Soil water measurements began on March 7, 2008 and ended on June 17, 2009.

In both Moraidi et al. (2015) and Nur Farahin's (2013) studies, the oil palm canopies had closed. Soil samples for the various aforementioned soil depths were randomly collected in the field and analysed for soil texture using the pipette method (Gee & Bauder, 1986) and soil organic matter by the combustion method (Skjemstad & Baldock, 2008) using the 412-Leco Carbon Auto-Analyzer.

Both Moraidi et al. (2015) and Nur Farahin (2013) did not measure leaf area index or the evaporative water losses via the soil and oil palm tree. Nonetheless, for closed oil palm canopies at 148-156 palms ha<sup>-1</sup>, their maximum leaf area index is approximately 6 m<sup>2</sup> m<sup>-2</sup> (Teh & Cheah, 2018) and total potential daily evapotranspiration is typically about 5 mm day<sup>-1</sup>, with 1 mm day<sup>-1</sup> for soil evaporation and 4 mm day<sup>-1</sup> for oil palm (Foong, 1999; Teh & Cheah, 2017; Teh et al., 2005). Consequently, in this study, these values for leaf area index ( $L$ ), potential soil evaporation ( $PET_s$ ), and potential tree transpiration ( $PET_c$ ) were used and assumed constant in the model.

### Model Validation

Model validation was carried out by comparing the overall degree of agreement between field soil water measurements with model simulations. For a given soil depth and day, the soil water content for the various replications was averaged and the mean compared with model simulations. Model accuracy was determined in two ways: visual inspection by plotting model simulations against measurements and using three goodness-of-fit statistical indexes: Normalised Mean Bias Error (NMBE), Normalised Mean Absolute Error (NMAE), and the revised Willmott's index of agreement ( $d_r$ ) (Willmott, Robeson, & Matsuura, 2012; Yu et al., 2006). These indexes are calculated as follows:

$$NMBE = \frac{\sum_{i=1}^N P_i - O_i}{\sum_{i=1}^N O_i} \quad (19)$$

$$NMAE = \frac{\sum_{i=1}^N |P_i - O_i|}{\sum_{i=1}^N O_i} \quad (20)$$

$$d_r = \begin{cases} 1 - p/2o & p \leq 2o \\ 2o/p - 1 & p > 2o \end{cases} \quad (21a)$$

$$p = \sum_{i=1}^N |P_i - O_i| \text{ and } o = \sum_{i=1}^N O_i - \bar{O}_i \quad (21b)$$

where  $P_i$  and  $O_i$  are the  $i$ -th pair of predicted and observed values, respectively ( $i = 1$  to  $N$  pairs); and  $\bar{O}$  is the mean of all observed values. NMBE (-1 to  $+\infty$ ) indicates a model's tendency to under- or overestimate relative to the mean observations. The larger the NME value, the larger the model's tendency for overestimation. NMAE (0 to  $+\infty$ ) indicates the mean absolute difference between predicted and observed values relative to the mean observations. Larger NMAE values indicate larger mean departures between model predictions and observations. The revised index of agreement  $d_r$  ranges between -1 and +1, where increasingly smaller positive or larger negative values indicate increasingly worse or inaccurate model predictions (particularly when  $d_r < 0$ ). For a perfect model, NMBE = 0 (no overall model bias), NMAE = 0, and  $d_r = +1$  (the latter

two indicating perfect agreement between model predictions and observations).

## RESULTS AND DISCUSSION

### Soil and Site Properties

Compared to the soil at UPM, the soil at Broga had a higher sand and lower clay content (Table 1). Overall, the soil at Broga was a sandy clay to sandy clay loam texture and at UPM a clay texture. The C content at Broga was also higher than that at UPM, most possibly due to differences between their management practices, where at Broga (a commercial oil palm estate), the oil palm fronds were pruned more regularly (once a month) and applied as a soil surface mulch at a higher rate than that practised at UPM (which was a non-commercial estate).

Broga was overall drier than UPM. The total rainfall at Broga was 3081 mm over 469 days of data collection, of which 241 days were rain days, and the mean rainfall per rain day was 12.8 mm. At UPM, the total rainfall over 167 days of data collection was 1890 mm, with 92 number of rain days and a mean of 20.5 mm per rain day.

Table 1  
Mean soil characteristics under oil palm at UPM (Nur Farahin, 2013) and Broga estate (Moraidi et al., 2015)

Estate/Property	Soil depth (cm)					
	0-15	15-30	30-45	45-60	60-75	75-90
<b>UPM</b>						
Clay (%)	47.7	53.5	55.2	58.3	57.0	58.9
Sand (%)	42.2	37.8	35.5	30.5	35.0	35.0
Organic C (%)	1.9	1.1	1.0	1.0	0.9	0.5
<b>Broga</b>						
Clay (%)	28.9	44.1	28.3	nd	nd	nd
Sand (%)	58.5	48.1	63.8	nd	nd	nd
Organic C (%)	2.7	1.8	1.5	nd	nd	nd

nd – not determined

**Model Accuracy**

Figure 4 to 6 show the degree of agreement between model simulations and measured soil water content. As expected, measured soil water content showed sharp increase

immediately after rainfall but during dry periods, soil water content declined in a more gradual manner. Model simulations likewise showed a similar trend to that observed for all soil depths (Figure 4 and 5).

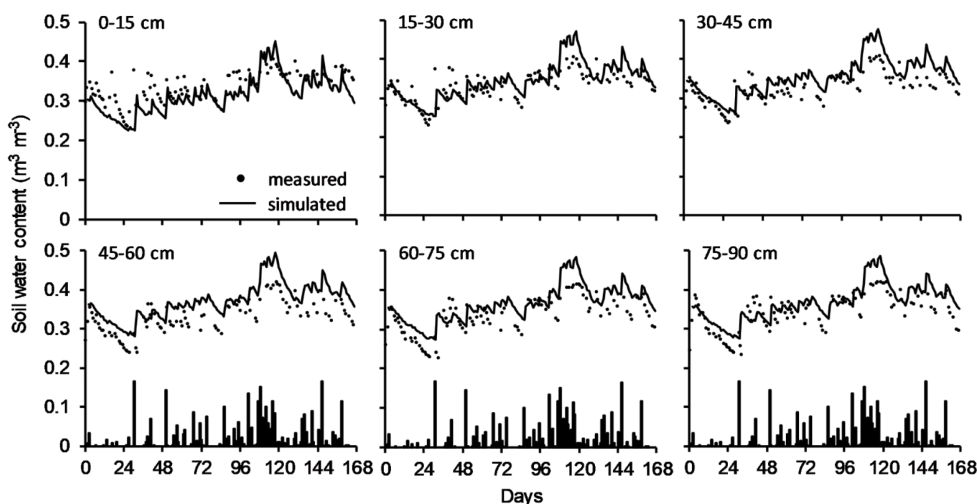


Figure 4. UPM Estate: Comparisons between model simulations and measured soil water content for six soil depths

Note. The bar charts at the lower panel show daily rainfall.

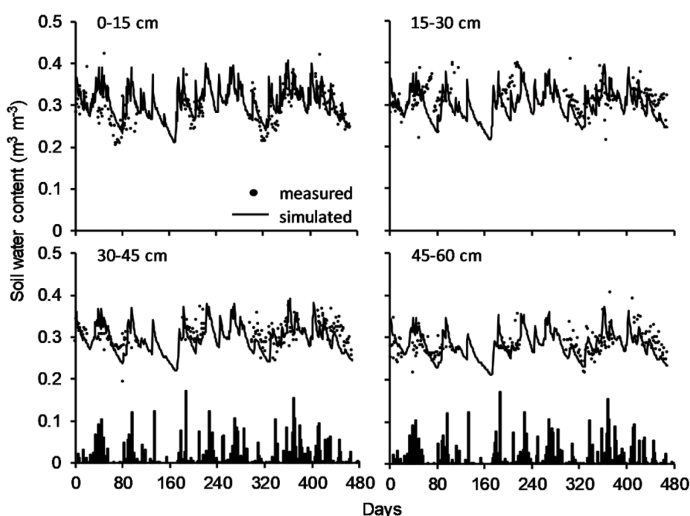


Figure 5. Broga Estate: Comparisons between model simulations and measured soil water content for four soil depths

Note. The bar charts at the lower panel show the daily rainfall

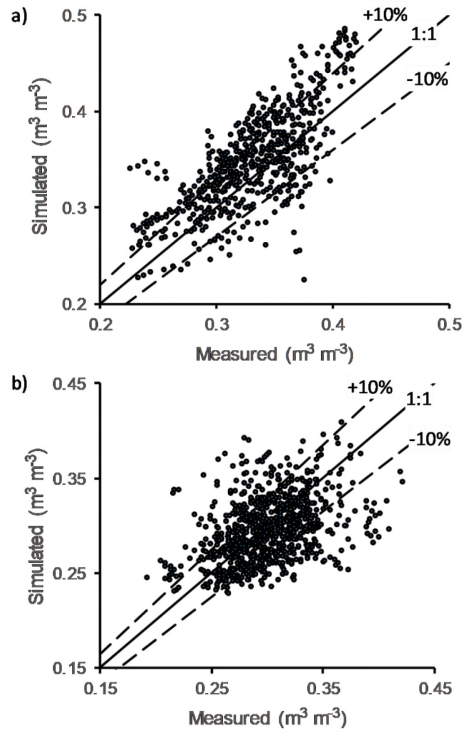


Figure 6. Overall degree of agreement between model simulations and measured soil water content for all soil depths at: a) UPM ( $N = 588$ ) and b) Broga ( $N = 1036$ ) Estate. The solid 1:1 lines indicate perfect agreement between model simulations and measured values, and the dashed lines indicate  $\pm 10\%$  deviation between simulation and measured values. For the UPM and Broga data sets, 282 (48%) and 1036 (56%) data points, are within the  $\pm 10\%$  lines respectively.

Overall, the degree of agreement between simulations and measurements was satisfactory. The NMAE, NMBE, and  $d_r$  goodness-of-fit indexes for simulations for the UPM site were 0.10, 0.05, and 0.53, respectively. There was a slight tendency of the model to overestimate the soil water content when the soil water content was  $0.40 \text{ m}^3 \text{ m}^{-3}$  or higher (Figure 6a); thus, giving a small positive NMBE value of 0.05, as mentioned earlier. For Broga, the values for NMAE, NMBE, and  $d_r$  were 0.10, -0.02, and 0.47, respectively. Compared to UPM, there was less model

bias for the Broga simulations (NMBE for Broga was -0.02 compared to 0.05 for UPM). The scatterplot in Figure 6b further shows no clear trend of an overall model bias in the Broga simulations. Nonetheless, the Broga simulations were slightly less accurate than the simulations for UPM. The  $d_r$  value for Broga was 0.47, slightly smaller than 0.53 as obtained for the UPM simulations. Figure 6 further shows a tighter or more linear clustering of points for the UPM (Figure 6a) than Broga (Figure 6b) simulations. Recall for a perfect model agreement,  $d_r$  is +1.0 and

increasingly smaller values, particularly negative values, indicate increasingly poor agreement between model estimates and measured values.

Finally, the NMAE values for both UPM and Broga were equal with each other at 0.10. In other words, on average, the absolute difference between model simulations and measured values of soil water content was only 10%.

Model simulations of soil water content could be improved if more accurate estimates or actual values of evapotranspiration (soil evaporation and plant transpiration) were given, rather than just assumed equal to 5 mm per day (partitioned to 1 and 4 mm for soil and tree, respectively), regardless of weather conditions for a given day. This means the model would require an energy balance model component to estimate the evaporative water loss from the soil and tree. Nonetheless, even without an energy balance component, the soil water simulations, at least for under closed oil palm canopies, were satisfactory, with little model bias and a small average model error.

Simulations of soil water flow are particularly sensitive to the estimations of unsaturated and saturated hydraulic conductivity (Eq. 7 and 8). Soil hydraulic conductivity is the highest when all the soil pores are filled with water. In other words, hydraulic conductivity is maximum at soil saturation. However, as the soil dries and the soil pores are gradually empty of water, hydraulic conductivity declines,

but this decline occurs not in a gradual but very rapid manner. For soils having a sandy clay loam or clay texture, like that used in this study, a 10% decline in their soil water content from saturation would result in about 10 times decline in their soil hydraulic conductivity. A 20% decline in soil water content from saturation would instead cause a decline in their hydraulic conductivity by 70 and 250 times for the sandy clay loam and clay soils, respectively. An early attempt in this study was to use the equation by Saxton and Rawls (2006) to estimate the saturated hydraulic conductivity, but model simulations of soil water content using this equation produced less accurate results than when the equation by Bittelli et al. (2015) (Eq. 8) was used in the soil water model. Other empirical equations to estimate hydraulic conductivity do exist (such as by Durner, 1994; Haverkamp et al., 1977; Kendy et al., 2003; Russo & Bresler, 1980), but they often require *a priori* knowledge on the values of one or more equation parameters that are not easily available or known, thus, making their use in the model of this study less attractive.

## CONCLUSIONS

The soil water model for oil palm was successfully developed and validated. The model was satisfactorily accurate, showing the same trend as that observed for the measured soil water content, rising rapidly immediately after rainfall and declining gradually during dry periods. Goodness-of-fit indexes indicated that the model

simulations showed little to no overall model bias and with an average prediction error (mean absolute difference between simulation and measured values) was only 10%. Model simulations could be increased if measured values of soil evaporation and tree transpiration values were provided in the model, but field measurements of evapotranspiration, especially for oil palm, can be challenging. Nonetheless, soil water model in this study can be coupled with an energy balance model component to provide more accurate estimates of evapotranspiration to improve simulation accuracy of soil water flow and content.

## REFERENCES

- Bentley, A. (2007). *Interception loss in Sedenak oil palm plantation*. (Unpublished undergraduate final year project report). Universiti Teknologi Malaysia, Skudai, Johor, Malaysia.
- Bittelli, M., Campbell, G. S., & Tomeu, F. (2015). *Soil physics with Python. Transport in the soil-plant-atmosphere system*. Oxford, UK: Oxford University Press.
- Carr, M. V. K. (2011). The water relations and irrigation requirements of oil palm (*Elaeis guineensis*): A review. *Experimental Agriculture*, 47(4), 629-652.
- Chong, S. Y. (2012). *Development of simple equations to estimate the net rainfall under closed tree canopies*. (Unpublished Masters dissertation). Universiti Putra Malaysia, Serdang, Selangor, Malaysia.
- Clemente, R. S., de Jong, R., Reynolds, W. D., & Hares, M. (1994). Testing and comparisons of three unsaturated soil water flow models. *Agricultural Water Management*, 25(2), 135-152.
- Corley, R. H. V., & Tinker, P. B. (2016). *The oil palm* (5th Ed.). Chichester, UK: Wiley-Blackwell.
- Damih, A. (1995). *Keberkesanan pemintasan air hujan oleh pokok kelapa sawit di dalam mengurangkan air larian permukaan* [Effectiveness of rainfall interception by oil palm trees in reducing surface runoff]. (B.Sc. final year project report). Skudai, Malaysia: Universiti Teknologi Malaysia.
- Durner, W. (1994). Hydraulic conductivity estimation for soils with heterogeneous pore structure. *Water Resources Research*, 30(2), 211-223.
- Foong, F. S. (1999). Impact of moisture on potential evapotranspiration, growth and yield of oil palm. In D. Arifin, K. W. Chan & S. R. S. A. Sharifah (Eds.), *Proceedings of the 1999 PORIM International Palm Oil Congress (Agriculture)* (pp. 265-287). Bangi, Malaysia: Palm Oil Research Institute of Malaysia.
- Gee, G. W., & Bauder, J. W. (1986). Particle-size analysis. In A. Klute (Ed.), *Methods of Soil Analysis. Part 1. Physical and Mineralogical Methods* (2nd Ed.) (pp. 363-375). Madison, WI: American Society of Agronomy-Soil Science Society of America.
- Haverkamp, R., Vauclin, M., Touma, J., Wierenga, P. J., & Vachaud, G. (1977). A comparison of numerical simulation models for one-dimensional infiltration. *Soil Science Society of America Journal*, 41(2), 285-294.
- Hillel, D. (1977). *Computer simulation of soil-water dynamics: A compendium of recent work*. Ottawa, Canada: International Development Research Centre.

- Kendy, E., Gerard-Marchant, P., Walter, M. T., Zhang, Y., Liu, C., & Steenhuis, T. S. (2003). A soil-water-balance approach to quantify groundwater recharge from irrigated cropland in the North China Plain. *Hydrological Processes*, 17(10), 2011-2031.
- Kropff, M. J. (1993). Mechanisms of competition for light. In M. J. Kropff, & H. H. van Laar (Eds.), *Modelling crop-weed interactions* (pp. 33-61). Wallingford, UK: CAB International
- Lee, C. T., & Izawanizam, A. (2013). Lysimeter studies and irrigation of oil palm in some inland soils of Peninsular Malaysia - Felda's experience. *The Planter*, 89(1042), 15-29.
- Lubis, M. E. S. (2016). *Water dynamics and groundwater quality assessment in an oil palm ecosystem*. (Unpublished doctoral thesis). Universiti Putra Malaysia, Serdang, Selangor, Malaysia.
- Miyazaki, T. (2005). *Water flow in soils*. Boca Raton, FL: CRC Press.
- Moraidi, A., Teh, C. B. S., Goh, K. J., Husni, M. H. A., & Fauziah, C. I. (2015). Effect of four soil and water conservation practices on soil physical processes in a non-terraced oil palm plantation. *Soil and Tillage Research*, 145, 62-71.
- Nelson, P. N., Banabas, M., Scotter, D. R., & Webb, M. J. (2006). Using soil water depletion to measure spatial distribution of root activity in oil palm (*Elaeis guineensis* Jacq.) plantations. *Plant Soil*, 286(1-2), 109-121.
- Nur Farahin, I. (2013). *Spatial and temporal change in soil water content in an oil palm estate*. (Unpublished undergraduate final year project). Universiti Putra Malaysia, Serdang, Selangor, Malaysia.
- Rey, H., Quencez, P., Dufrière, E., & Dubos, B. (1998). Oil palm water profiles and water supplies in Côte d'Ivoire. *Plantations, Recherche, Développement*, 5(1), 47-57.
- Russo, D., & Bresler, E. (1980). Scaling soil hydraulic properties of a heterogeneous field soil. *Soil Science of America Journal*, 44(4), 681-684.
- Saxton, K. E., & Rawls, W. J. (2006). Soil water characteristic estimates by texture and organic matter for hydrologic solutions. *Soil Science Society of America Journal*, 70(5), 1569-1578.
- Skjemstad, J. O., & Baldock, J. A. (2008). Total and organic carbon. In M. R. Carter & E. G. Gregorich (Eds.), *Soil sampling and methods of analysis* (pp. 225-237). Boca Raton, FL: CRC Press.
- Teh, C. B. S. (2006). *Introduction to mathematical modeling of crop growth: How the equations are derived and assembled into a computer program*. Boca Raton, FL: Brown Walker Press.
- Teh, C. B. S., & Cheah, S. S. (2018). Modelling crop growth and yield in palm oil cultivation. In A. Rival (Ed.), *Achieving sustainable cultivation of oil palm* (pp. 183-227). Cambridge, UK: Burleigh Dodds Science Publishing.
- Teh, C. B. S., Henson, I. E., Harun, H., Goh, K. J., & Husni, M. H. A. (2005). Modelling oil palm growth and yield. In C. B. S. Teh, O. H. Ahmed, C. I. Fauziah, A. Izham, W. D. Wan Noordin, & Z. Z. Zakaria (Eds.), *SOILS 2005: Advances in soil science for sustainable food production. Proceedings of the Malaysian Society of Soil Science 2005* (pp. 204-206). Serdang, Malaysia: Malaysian Society of Soil Science.
- van Keulen, H., & Seligman, N. G. (1987). *Simulation of water use, nitrogen and growth of a spring wheat crop*. Simulation Monographs. Wageningen, The Netherlands: Pudoc.
- Willmott, C. J., Robeson, S. M., & Matsuura, K. (2012). A refined index of model performance. *International Journal of Climatology*, 32(13), 2088-2094.

- Yu, S., Eder, B., Dennis, R., Chu, S. H., & Schwartz, S. E. (2006). New unbiased symmetric metrics for evaluation of air quality models. *Atmospheric Science Letters*, 7(1), 26-4.
- Zulkifli, Y., Geoffery, J., Saw, A. L., & Norul, S. T. (2006). Preliminary study on throughfall spatial variability and stemflow characteristics under oil palm catchment. In *Proceedings of the National Water Conference* (in CD). Kuala Lumpur, Malaysia: Malaysian Hydrological Society.